DNA-based AND logic gate as a molecular precision tool: selective recognition of protein pairs in lipid nanodiscs and subsequent binding of gold nanorods

S. De[1#], M. Hechler[2#], M. Cheng[1], H. Giesler[2], S. Brandau[3], B. Sacca[1*], S. Schlücker[2*]

[#]equal contributors

*corresponding authors

[1]Department of Biology, Center for Medical Biotechnology (ZMB) and Center for Nanointegration Duisburg-Essen (CENIDE), Universitätsstr. 5, D-45141 Essen, Germany, email: barbara.sacca@uni-due.de

[2]Department of Chemistry, Center for Medical Biotechnology (ZMB) and Center for Nanointegration Duisburg-Essen (CENIDE), Universitätsstr. 5, D-45141 Essen, Germany email: sebastian.schluecker@uni-due.de

[3]Experimental and Translational Research,Department of Otorhinolaryngology, University Hospital Essen, 45147 Essen, Germany

Abstract

The specificity of target recognition is paramount in fields such as cellular biology, diagnostics, and therapy. Traditional antibody-based methods focus on recognizing single antigens; however, the next level of specificity involves targeting pairs of antigens simultaneously. This study introduces a DNA-based molecular logic AND gate designed to recognize the two membrane proteins PD-L1 and CD3 as antigens via the corresponding antibody-oligonucleotide conjugates. The two membrane proteins are embedded in lipid nanodiscs that serve as a model system for cell membranes. By utilizing antibody-oligonucleotide conjugates as input signals, the DNA logic gate operates sequentially, becoming fully activated only upon binding both target proteins. The output signal facilitates subsequent actions, such as target isolation via magnetic bead extraction and functionalization with DNA-tagged gold nanorods for potential photothermal therapy. Our proof of concept for a molecular precision tool that processes two input signals in an AND operation and converts them to an output signal offers new avenues for high-specificity diagnostics and therapeutic interventions.

Introduction

Achieving specificity by target-specific recognition elements is important in many scientific areas including cellular biology, diagnostics, and therapy. To this end, antibodies are routinely used for antigen recognition. The next level of increased specificity is to selectively target structures that do not only contain one particular antigen, A *or* B, but pairs of antigens: A *and* B. Simultaneous binding of two targets can be achieved for example using a bivalent construct with high positive cooperativity.[1] This construct is composed of the antibody against A (aA) and the antibody against B (aB) anchored to the same scaffold through a molecular linker. In this scenario, bivalent binding can be achieved when the overall binding affinity of the construct for A and B is greater than the sum of the affinities against each individual antigen: “only A” or “only B”.[2, 3] Often, however, mono- and bivalent complexes coexist in solution and may be difficult to distinguish or isolate. In contrast, sequential recognition processes can be designed to enable binding to B only if binding to A has already occurred, resulting in the selective targeting of pairs of A and B in spatial proximity. Such reaction cascades can be realized using so-called molecular logic AND operators.[4-6]

Over the last years, a multitude of advances have been done to engineer molecular Boolean gates that execute AND, OR, NOT, NOR, XOR or NAND operations.[5, 7, 8] This development has been driven by the search of alternative means to control for example gene expression or protein functioning for applications in bionanotechnology and medicine.[9-15] Differently from molecular[16, 17] and protein-based logic gates[18], DNA-based devices are easily programmable as they rely on the predictable Watson-Crick base pairing rule. This, together with the high thermodynamic stability of the DNA and its synthetic accessibility at low costs, make it an ideal candidate for the construction of logic gates.[7, 19, 20]

DNA logic gates essentially perform logical operations at the molecular level. Upon recognizing specific single-stranded oligonucleotides (the "input" signals), a DNA logic gate undergoes a series of conformational transitions, hybridizations, and strand exchanges, leading to the production of an "output" signal. This cascade of reactions follows a programmable sequential order, which is governed by toehold-mediated strand displacement (TMSD) mechanisms.[21, 22] In particular, a "two-input" AND gate functions by producing an output signal only if both inputs are present. Input signals can be linked to ligands or antibodies to enable the DNA device to recognize the simultaneous presence of two specific targets. The output signal is typically a single-stranded DNA that can be in turn exploited to "translate" the molecular recognition event into an action: e.g. by binding to a DNA-tagged fluorophore for bioimaging or diagnostics[9-15] or – as presented here – by binding to a DNA-tagged gold nanorod (AuNR) for later use in photothermal therapy (PTT).[23, 24]

The DNA AND logic gate employed in this work is schematically illustrated in Figure 1. The logic gate operation in this manuscript is performed purely in solution. The device is designed to specifically sense two different cell surface receptors: the human recombinant PD-L1[25] and the δ/ε-domain of CD3.[26, 27] These represent the A and B target antigens of our system. Since these are transmembrane proteins, their correct formation and stability is supported by embedding them into lipid nanodiscs.[28, 29] Antibodies specifically raised against PDL1 (anti-PDL1) and CD3 (anti-CD3) are then covalently linked to DNA strands, resulting in two distinct types of oligonucleotide-antibody conjugates, aA and aB. In the first step of the reaction cascade, these conjugates selectively recognize the target membrane proteins (step 1 in Fig. 1). Each conjugate displays a unique DNA strand that functions as one of the two input signals of the DNA logic gate. Upon binding of the DNA logic gate to the first input signal (step 2), a priorly blocked region of the logic gate becomes accessible for binding of the second input signal (step 3). This results in the fully opened logic gate bound to both proteins, with each protein being embedded in a nanodisc (step 4). At this stage, the logic gate presents an accessible single-stranded region that can be used for isolation of the desired pair of targets by magnetic bead extraction (step 5). In the final step (step 6), a TMSD reaction is employed to functionalize the pair of desired targets with a gold nanorod. In future studies, this construct shall be used as a therapeutically active agent to eliminate the target cells by photothermal therapy.

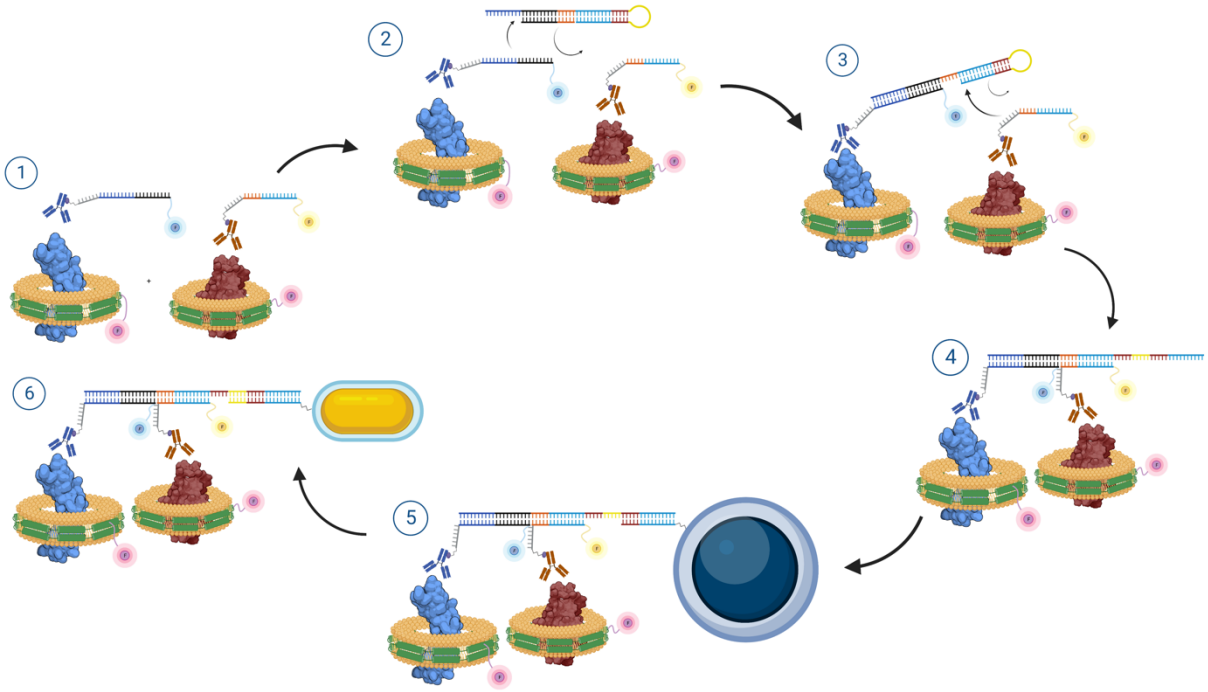

Figure 1. Schematic overview of the DNA logic gate operation in combination with all employed input and output components. Step 1 depicts the membrane protein binding by monoclonal antibodies covalently coupled to the input DNA strands necessary for logic gate operation. The proteins of interest are inserted into separate lipid nanodiscs. In step 2, the binding of the first input strand to the logic gate takes place, displacing the before hybridized oligonucleotide and partially opening the gate. In step 3, the binding of the second input strand to the newly accessible toehold region can be seen, which then fully opens the DNA logic gate. The illustration from step 4 visualizes the fully opened logic gate with the two respective antibodies and bound proteins. In step 5, the hybridization of opened logic gate and the complementary output sequence, coupled to a magnetic bead, takes place. This construct was used for fluorescence intensity measurements detecting the respective fluorophores of the tagged components. In the final step 6, a strand displacement reaction by a longer complementary output DNA sequence bound to a AuNR takes place, removing the magnetic bead from the logic gate and resulting in the final construct of the study.

In conclusion, we present an approach to selectively recognize a pair of transmembrane proteins using a DNA logic gate that performs an AND operation. In our system, the antibody-oligonucleotide conjugates play the role of recognition units and input signals, while the DNA logic gate is the molecular processing unit that transforms the inputs into an output signal. This latter is ultimately used to perform a specific action on the target molecules, being this either a purification or a labelling. We envision that this approach can be used as a high precision molecular tool for sensing, transmitting, and translating molecular information.

Results and Discussion

Design of the DNA AND logic gate and characterization of its functioning.

To execute the intended AND logic operation, the DNA logic gate was designed to adopt a closed hairpin loop conformation in absence of the input strands (Figure 2A). The designed AND gate consists of two oligonucleotides (**a** and **b**) hybridizing into three major domains: a central duplex (in black, orange, light blue and red), a single-stranded hairpin loop (yellow) and a single-stranded toehold-binding region (dark blue). Binding of the first input strand (**c**) to the toehold region of the logic gate (state i) results in the detachment of strand **b** and concomitant presentation of a different single-stranded region (state ii). This latter is the toehold for recognition and binding of the second input strand (**d**). Hence, the consecutive hybridization of the two input strands, **c** and **d**, leads to opening of the logic gate, which essentially corresponds to the successful implementation of the AND operation (state iii). This reaction makes a previously inaccessible region now available for further hybridization with a complementary oligonucleotide (**e**), forming the last species of the reaction cascade (state iv). In other terms, this last step enables to employ the AND logic operator to perform a desired action on the selected pair of target molecules. In this work, we used this last step to target and combine a pair of transmembrane proteins and label them with a AuNR.

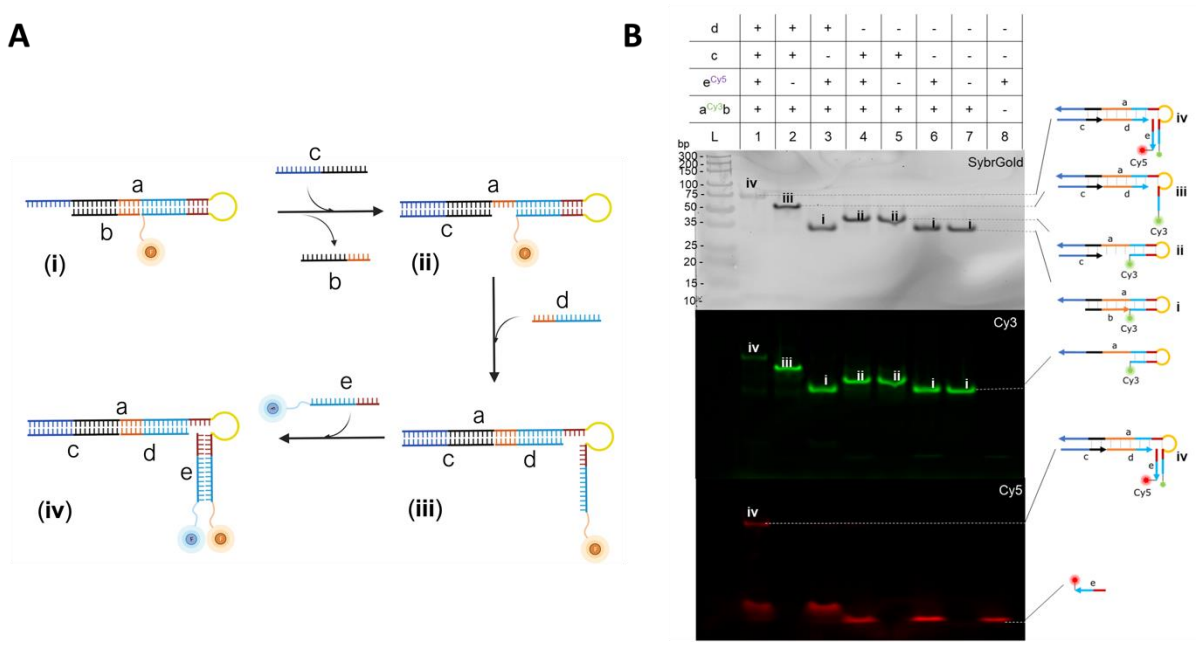

Figure 2. Overview of the programmed logic gate strand displacement reactions. In **A**, a scheme depicts each step, starting with the closed logic gate carrying a Cy3 fluorophore. Firstly, oligonucleotide **c** replaces strand **b** and initiates the partial logic gate opening. Due to a new accessible toehold region, oligonucleotide **d** can bind and fully open the hairpin loop of the gate. In the last step, output oligonucleotide **e**, carrying a Cy5 fluorophore, hybridizes to its respective output region on the gate. In **B**, an image of a native PAGE analysis of each reaction step is depicted. The first gel image depicts the SybrGold staining of the gel, visualizing every present component. In the two lower images, the fluorescence signals of Cy3 and Cy5 are shown. It can be concluded that the addition of oligonucleotides always results in the expected shift due to a slower migration through the gel and that the binding reactions take place with high product yields. Unspecific opening if only one input oligonucleotide is present could hardly be detected, which means the DNA logic gate operates in the desired manner.

The individual steps of the reaction cascade were all performed in solution and characterized by native PAGE using fluorescently labelled oligonucleotides (Figure 2B). The binding of input strand **c** to the logic gate was confirmed by the appearance of a molecular species of higher molecular weight and correspondingly lower migration rate (from state i to ii, lanes 7 to 4). Binding of strand **d**, in absence of strand **c**, had no effect (lane 3); whereas only the presence of both input strands led to opening of the loop (lane 2, state iii). Finally, addition of oligo **e** to the open logic gate resulted in formation of a molecular species with the highest molecular weight and slowest migration rate (lane 1, state iv). Altogether, these data demonstrate that the logic gate works as intended and that the binding of the first input is required for the recognition and binding of the second input: that is, the AND gate relies on a defined sequential order of reactions. Moreover, our data show that the AND operation of the DNA device can be used to tag the selected pair of inputs for downstream applications, e.g., using a fluorescently labelled oligo for tracking purposes. Importantly, the presence of oligo **e** in the initial reaction mixture did not affect the functioning of the device, indicating the robustness of the design and the absence of leakage or spurious reactions.

DNA-antibody conjugation and characterization

To enable the DNA logic gate to selectively target the desired pair of membrane proteins out of a reaction mixture, the input strands were covalently linked to monoclonal antibodies and the resulting DNA-antibody conjugates were implemented into the construct as targeting agents. The oligonucleotides **c** and **d** were covalently linked, respectively, to the Fc-region of the antibody against PDL1 (antiPDL1) and CD3 (antiCD3), using the commercially available oYo-link® reagent. This reagent is a heterobifunctional crosslinker: one side of the molecule consists of high-affinity antibody-binding domains and contains a photo-crosslinker within the Fc-binding site, the other side of the molecule displays an DBCO group for further conjugation using click chemistry. Upon UV illumination, the oYo-link was covalently bound to the Fc-region of the antibody. Beforehand, the linking reagent was treated with an azide-modified oligonucleotide. Successful formation and isolation of the desired conjugates (**c**-antiPDL1 and **d**-antiCD3) was validated by SDS-PAGE (Figure 3A) and anion exchange chromatography (Figure 3B), using a fluorescently labelled oligonucleotide. The operation of the logic gate was then tested using the DNA-antibody conjugates as input signals. For this purpose, a solution containing the DNA logic gate and the oligo **e**, fluorescently labelled, respectively, with Cy3 and Cy5, was incubated with both DNA-antibody inputs, **c**-antiPDL1 and **d**-antiCD3. Single-stranded **c** and **d** inputs were used as controls. Correct AND functioning of the gate is expected to lead to hybridization of the oligo **e** to the open logic gate, eventually resulting in a strong FRET signal between the donor and acceptor dyes.

Hence, the change of FRET over time was monitored upon addition of the inputs (Figure 3C). Addition of the DNA-antibody conjugates led to a slower FRET change as compared to the same reaction triggered by DNA-only inputs (cfr. blue and orange curves with grey curve in Fig. 3C). In particular, whereas the DNA-antibody conjugates from fraction 2 resulted in overall reduced logic gate opening, the conjugates from fraction 3 opened the logic gate with similar efficiency as the DNA-only containing controls. All in all, these data indicate that the coupling of DNA oligonucleotides to large molecules such as antibodies does not impair the logic gate operation.

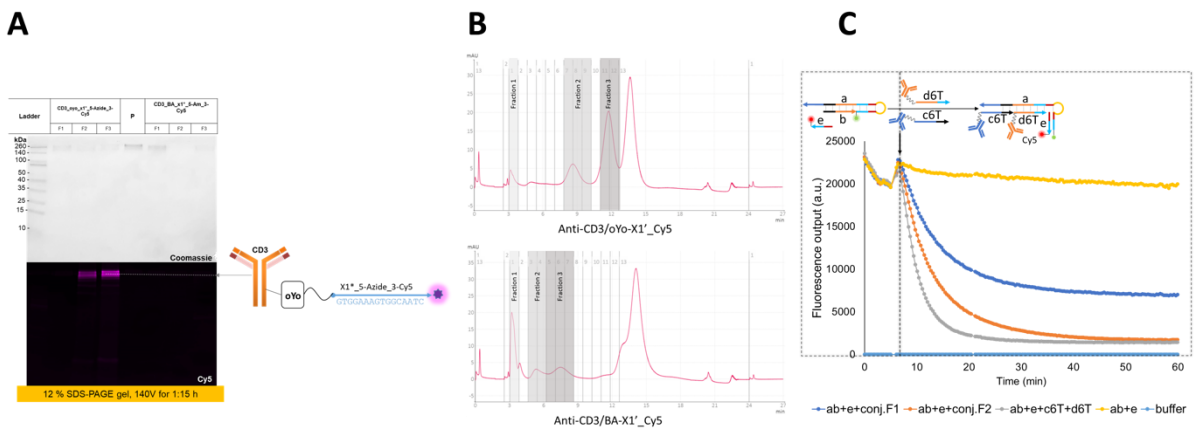

Figure 3. Investigation of DNA-antibody conjugate binding to the DNA logic gate. **A** depicts gel images after SDS-PAGE analysis of conjugated samples and successive Coomassie staining. Colocalization of the protein signal and the fluorescent signal from the DNA suggests that the conjugation reaction was successful. In **B**, a chromatogram of an anion-exchange chromatography for separation and analysis purposes of the conjugates is depicted. The first peak, labelled fraction 1, indicates the free protein eluting from the column. In the second (fraction 2) and third (fraction 3) peaks, the DNA-antibody conjugates elute. The fractions are labelled in accordance with their gel application from **A**. The fourth peak indicates the elution of pure oligonucleotides from the column. Thus, a successful separation can be concluded. In **C**, the employment of purified DNA-antibody conjugates as input strands compared to respective controls is depicted. The fluorescence intensity measurement indicates successful hybridization of the input strands to the logic gate, even if the big antibodies are conjugated to the short DNA strands.

Protein embedding into lipid nanodiscs

To mimic a cell membrane system, human recombinant membrane proteins PD-L1 and CD3 were incorporated into lipid nanodiscs. Membrane proteins are a key conduit for cell communication, molecule transport, cell recognition or energy production. However, their usage in aqueous solutions is limited due to destabilization of the structure and impaired functionality in absence of a lipophilic environment. Thus, nanodisc technology possesses the potential to enable valuable studies on and with the otherwise insoluble proteins.[30] Here, the lipid nanodiscs are stabilized by their scaffolding protein MSP1D1, building dimers and forming an encircling amphipathic belt around the employed phospholipids, resulting in a discoidal formation with a diameter of 10 nm and a height of 4 nm. Primary analysis and purification were performed via size exclusion chromatography (SEC). The chromatograms indicated the formation of constructs with the desired size; moreover, the self-assembled constructs could be separated from residual sample components (Figure S1). To investigate if the constructs in the eluted fractions possess the desired shape, transmission electron microscopy was performed. Negative staining revealed a high-yield formation of discoidal structures with a diameter of 12.24±1.45 nm and a height of 4.51±0.32 nm (Figure 4B). These dimensions deviate from the values reported in the literature (diameter of 9.5 nm and height of 4.2 nm), probably due to nanodisc structure collapse during sample preparation. The lipid nanodiscs can either be seen from a top or side view. Lipid nanodiscs visible from the side tend to “stack” with other nanodiscs, thus leading to the aligned formations that can be seen in Figure 4D. This effect can occur when positively charged ions from the buffer partly mask the negative surface charge of the lipid nanodisc, resulting in coaxial stacking of the discoidal structures.

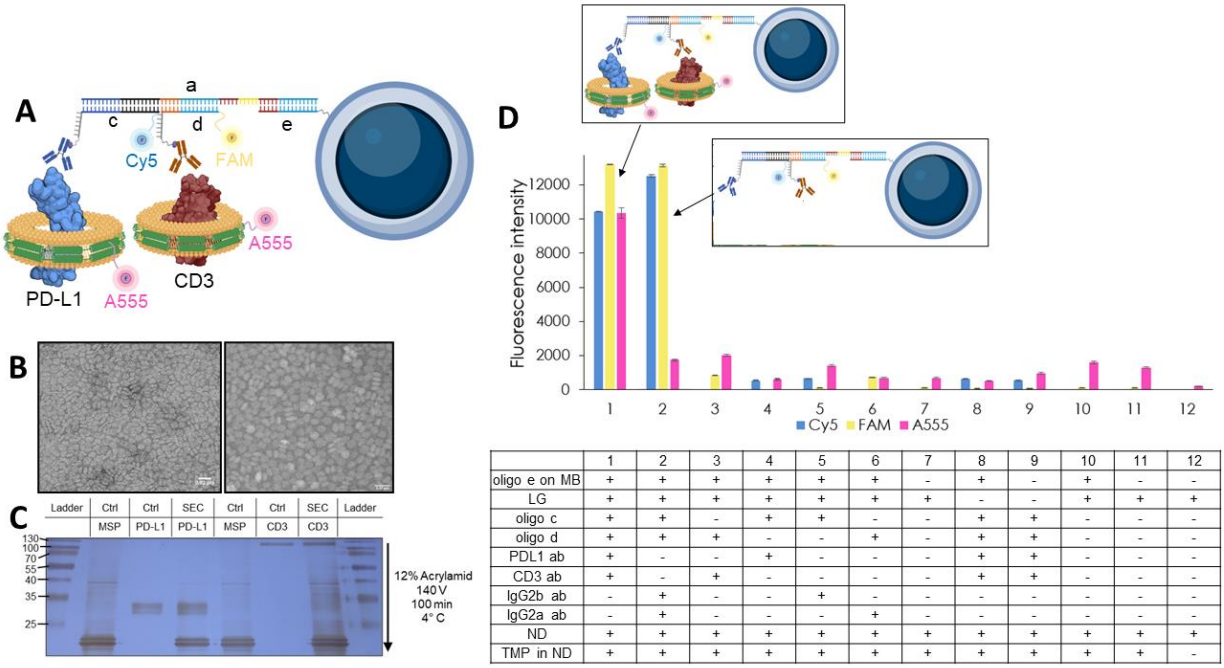

	1	2	3	4	5	6	7	8	9	10	11	12
oligo e on MB	+	+	+	+	+	+	-	+	-	+	-	-
LG	+	+	+	+	+	+	+	-	-	+	+	+
oligo c	+	+	-	+	+	-	-	+	+	-	-	-
oligo d	+	+	+	-	-	+	-	+	+	-	-	-
PDL1 ab	+	-	-	+	-	-	-	+	+	-	-	-
CD3 ab	+	-	+	-	-	-	-	+	+	-	-	-
IgG2b ab	-	+	-	-	+	-	-	-	-	-	-	-
IgG2a ab	-	+	-	-	-	+	-	-	-	-	-	-
ND	+	+	+	+	+	+	+	+	+	+	+	+
TMP in ND	+	+	+	+	+	+	+	+	+	+	+	-

Figure 4. Elucidation of the magnetic bead binding assay employing the logic gate. **A** depicts the construct that is able to bind to the magnetic bead covered with output oligonucleotide **e**. In **B**, uranyl acetate-stained TEM images of lipid nanodiscs after SEC separation are depicted. The formed lipid nanodiscs have a round form if seen from the top and an elongated oval shape if seen from the side view. The structures display a diameter of 12.24±1.45 nm and a height of 4.51±0.32 nm. An image of a silver nitrate stained SDS-PAGE analyzing SEC-separated membrane protein carrying nanodisc samples compared to respective controls is shown in **C**. The presence of the desired membrane proteins as well as the encircling membrane scaffolding protein can be seen according to the migration behaviour of the present proteins in the respective lanes 4 and 6. In **D**, the fluorescence intensity of washed samples containing the components indicated in the table below is shown, implicating successful logic gate and nanodisc binding to the magnetic beads, as well as little unspecific binding.

In the next step, the protein composition of the eluted fractions was analyzed via SDS-PAGE (Figure 4C). After gel electrophoresis, the gels were stained with an adjusted silver nitrate staining protocol for proteins. The eluted fractions (SEC lanes 4 and 7) indicated the presence of both the encircling membrane scaffolding protein (MSP) and the respective membrane protein of interest. Impurities and unexpected bands were present both in the MSP and the PD-L1 controls, which could stem from incomplete tag digestion after enrichment by the providing companies. The band of the CD3-fusion protein migrated higher than expected from literature reports, even after glycosylation. However, since the bands in the analysed fraction samples all migrate in accordance with their respective controls, it is highly probable, that all the desired proteins are present in the nanodisc fractions. This conclusion is also corroborated by the functional tests with our molecular precision tool (vide infra). Nevertheless, we cannot provide experimental data that indicate the exact position and orientation of the membrane protein within the nanodiscs.

Application of the AND logic gate for action on a selected protein pair

The final goal of this study was to use the AND logic operation of the DNA device to perform a desired action on a selected protein pair. As a proof-of-principle, we employed the AND logic gate for extracting the protein pairs from a reaction mixture and further labelling them with a

AuNR. For this purpose, magnetic beads with a carboxyl group presenting surface were conjugated to amino-modified oligo **e** via EDC/sNHS chemistry. After three washing steps, the so-modified magnetic beads were incubated with a solution of logic gate pre-treated with DNA-antibody conjugates, either in presence or absence of the corresponding nanodisc-embedded proteins. Control samples were prepared to test the reliability of the magnetic beads mediated pull-down assay. The full set-up consisted of the following components: the AND logic gate, the first and second inputs, which are fluorescently labelled at the DNA strands **c** and **d**, respectively, with a Cy5 and a FAM dye, and two types of Alexa555-labeled nanodiscs carrying either PD-L1 or CD3. Thus, whereas the co-presence of Cy3 and Cy5 signals is an indication of successful logic gate operation, the additional presence of Alexa555 signal demonstrates that the device can be effectively used for targeting the desired protein pair. The data obtained by the pull-down assay are reported in Figure 4D and indicate that both the operation of the logic gate (sample 2) and its binding to the embedded proteins (sample 1) worked as expected. Residual unspecific binding of single oligonucleotides as well as lipid nanodiscs were observed in the control samples; however, unspecific logic gate operation did not occur.

In the next step, the logic gate construct was released from the magnetic bead and linked to a AuNR for potential use in photo-thermal therapy. To achieve this, AuNR-DNA conjugates were synthesized that contained an oligonucleotide sequence (**e_long**) fully complementary to the logic gate but longer than the regular strand **e**. Sequence **e_long** can therefore displace sequence **e** from the open logic gate forming a longer and more stable duplex. This results in the removal of the logic gate from the magnetic bead and its further binding to the AuNR. Firstly, AuNR with an absorbance maximum at 808 nm were synthesized in a wet-chemical modified seeded approach from González-Rubio *et al.* and further functionalized.[31] The absorbance was tuned to 808 nm due to the later envisioned use of the logic gate for optimized targeting in photothermal therapy. Analysis of the successful fine-tuning of the absorbance was performed via UV-Vis absorption spectroscopy (Figure S2). The size and yield of the synthesized samples were analyzed via transmission electron microscopy (Figure 5B). The AuNR were coated with a 5 kDa PEG-COOH shell. Either **e** or **e_long** oligonucleotides containing a terminal amino group were conjugated to the AuNR surface after activation of the PEG-COOH groups via EDC/sNHS chemistry. Measurements of the hydrodynamic radius and ζ-potential (see Figure 5C) indicated the successful surface modification with the intended oligonucleotides.

Upon addition of the two input strands, **c** and **d**, the open logic gate was treated with AuNR-DNA conjugates covered with oligo **e**. The same experiment was repeated using oligo **e** or AuNR-only samples and the quenching of the fluorescence signal was monitored over time (Figure 5D). We hypothesized that, when compared to the AuNR alone, the AuNR-DNA conjugates successfully bound to the open logic gate would result in a significant drop of the fluorescence signal. Indeed, in this case, the AuNR would be placed in close proximity to the Cy3 fluorophore via hybridization of the conjugated **e** strands to the opened logic gate. The results show that the AuNR-DNA conjugates significantly reduced the emitted fluorescence of the logic gate as compared to a control with only AuNR (blue vs. orange curve in Fig. 5D). However, binding of Cy5-labelled oligo **e** alone led to a more striking quenching effect, suggesting that conjugation of **e** to the AuNR might hinder the next hybridization step. Possible explanations for this could be steric hindrance by the big PEG-coated AuNR construct (compared to the size of the oligonucleotide strands) or by less efficient quenching of the AuNR as compared to the Cy5 fluorophore. However, it can be concluded that the conjugation of AuNR to **e** does not prohibit strand hybridization, and thus AuNR-DNA conjugates can be employed for further experiments on the selected membrane proteins.

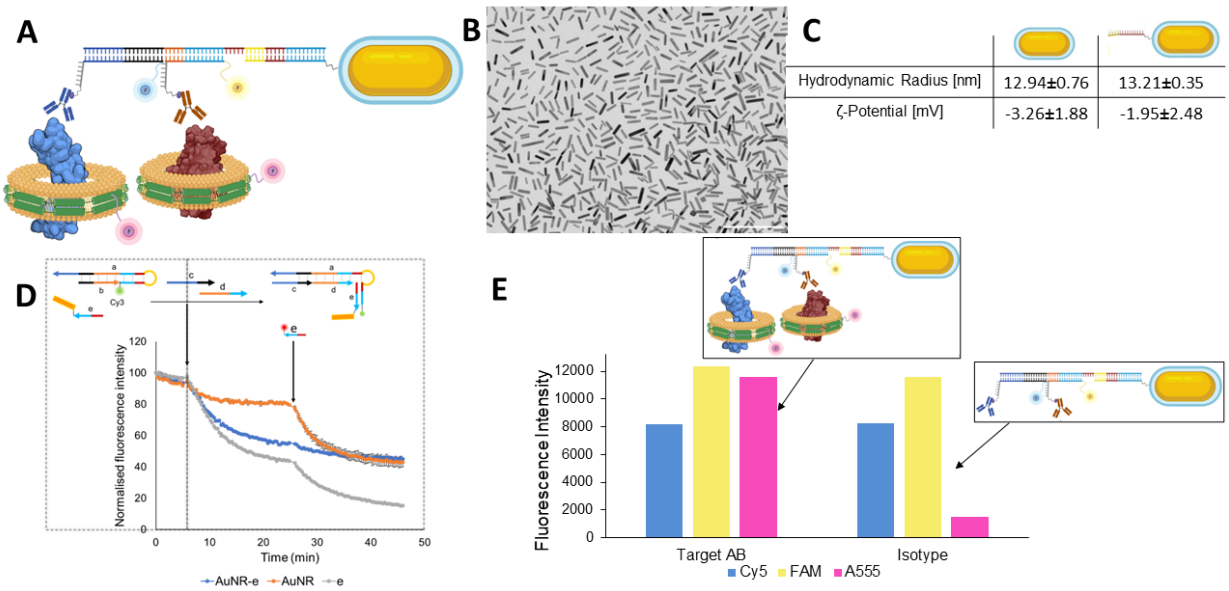

Figure 5. Analysis overview of the strand displacement reaction replacing the magnetic bead with a AuNR coupled to a longer output oligonucleotide. **A** is a scheme illustrating the final construct. In **B**, a TEM image of the employed 24 nm long bare AuNR is shown, **C** displays the results of hydrodynamic radius and ζ-potential measurements indicating minor size and surface charge changes after oligonucleotide conjugation. In D, further insight into the strand displacement reaction is gained, as it shows the fluorescence intensity changes over time after the addition of AuNR conjugated output oligonucleotides. Due to the natural quenching of fluorescence by AuNR to fluorophores in close proximity to the nanoparticles, the decline of fluorescence after the addition of AuNR-DNA conjugates indicates successful binding to the opened logic gate. An addition of a different quenching oligonucleotide shows little change in the fluorescence intensity containing the AuNR-DNA conjugates, but successful quenching in the other two control samples. This is another indication for successful AuNR-DNA binding to the opened logic gateIn image E, the fluorescence intensity of centrifuged samples after performing the strand displacement reaction are shown. Centrifugation separates the magnetic beads from the AuNR and only fluorescence emitted from logic gate and lipid nanodisc components bound to the AuNR can be detected in these samples. This indicates a successful strand displacement reaction.

The final experiment aimed at demonstrating the integrity and functionality of our entire molecular precision tool comprising both recognition unit (antibody-DNA conjugates) and processing unit (DNA AND logic gate) as well as its binding capacity to the AuNR-DNA conjugate for future applications in photothermal therapy. To this end, we hypothesized that upon addition of AuNR-DNA conjugates covered with the **e_long** sequence, the entire construct should be released from the magnetic beads via DNA strand displacement mechanisms. After incubation, the magnetic beads were separated from the AuNR with a magnet. Subsequently, both the magnetic beads as well as the AuNR were washed three times. Finally, the fluorescence intensities of the respective samples were measured (Figure 5E). The results showed that whereas the magnetic beads samples contained only residual fluorescence, the AuNR samples emitted high fluorescent signals, indicating the presence of all desired components, and thus the successful displacement of the entire construct from the magnetic beads. Altogether, our data demonstrate that the desired pairs of nanodisc-embedded membrane proteins could be fished from a reaction mixture using antibody-DNA conjugates as the inputs of an AND DNA logic gate and that the subsequent “linking” of the construct to PTT-ready AuNR could be performed successfully.

Conclusion

To summarize, we here report on a molecular precision tool comprising two antibody-DNA conjugates as molecular recognition units for two transmembrane proteins embedded in lipid nanodiscs and a DNA-based AND logic gate as the molecular processing unit. This approach is capable to recognize and bind pairs of transmembrane proteins in close proximity (up to ca. 10 nm). Importantly, the final construct can be further used to tag the selected pair of proteins with a AuNR for potential applications in diagnostics and therapy, for example, based on photothermia. Since the logic gate is responsive to pre-designed single stranded input signals, these latter can be in principle conjugated to virtually any type of antibody, enabling to apply the same logic gate to a different pair of proteins. We also demonstrated that lipid nanodiscs help to stabilize transmembrane proteins, without affecting the DNA logic gate operation. Hence, our approach offers a versatile molecular precision tool for the selected recognition, isolation, and tagging of desired protein pairs. Further implementation of DNA logic operators may enable to perform different types of operations on pairs or even multiple target molecules.

Acknowledgements

The German Cancer Aid (Deutsche Krebshilfe, DKH) financially supported this study with a research grant (Visionäre neue Konzepte in der Krebsforschung: Präzisionsimmuntherapie durch DNS-Logikgatter-Erkennungsmotive auf Goldnanostäbchen). Moreover, we thank the Imaging Center Essen (IMCES) at the Department of Medicine of the University of Duisburg-Essen, for providing access to its electron microscope imaging services, specifically the JEOL JEM 1400 Plus. The proFIRE® separation device was funded by the German Research Foundation (Deutsche Forschungsgemeinschaft, DFG) via the collaborative research center CRC1093 (Supramolecular Chemistry of Proteins).

References

1. Mammen, M., Choi, S.K. & Whitesides, G.M. Polyvalent Interactions in Biological Systems: Implications for Design and Use of Multivalent Ligands and Inhibitors. *Angew Chem Int Ed Engl* **37**, 2754-2794 (1998).
2. Kitov, P.I. & Bundle, D.R. On the nature of the multivalency effect: a thermodynamic model. *J Am Chem Soc* **125**, 16271-16284 (2003).
3. Jingjing, M.A. Three-input logic gate based on DNA strand displacement reaction. *Sci Rep* **13**, 15210 (2023).
4. Okamoto, A., Tanaka, K. & Saito, I. DNA Logic Gates. *J Am Chem Soc* **126**, 9458-9463 (2004).
5. Yin, F., Wang, F., Fan, C., Zuo, X. & Li, Q. Biosensors based on DNA logic gates. *VIEW* **2**, 20200038 (2021).
6. Zhang, Y., Hu, N., Xu, J. & Wang, Z. DNA logic programming: From concept to construction. *VIEW* **5**, 20230062 (2024).
7. Wang, F. et al. Implementing digital computing with DNA-based switching circuits. *Nat Commun* **11**, 121 (2020).
8. Emanuelson, C., Bardhan, A. & Deiters, A. DNA Computing: NOT Logic Gates See the Light. *ACS Synth Biol* **10**, 1682-1689 (2021).
9. Chang, X. et al. Construction of a Multiple-Aptamer-Based DNA Logic Device on Live Cell Membranes via Associative Toehold Activation for Accurate Cancer Cell Identification. *J Am Chem Soc* **141**, 12738-12743 (2019).

10. Chen, J., Fu, S., Zhang, C., Liu, H. & Su, X. DNA Logic Circuits for Cancer Theranostics. *Small* **18**, 2108008 (2022).
11. Gong, H., Dai, Q. & Peng, P. Cell-Membrane-Anchored DNA Logic-Gated Nanoassemblies for In Situ Extracellular Bioimaging. *ACS Appl Mat Inter* **14**, 43026-43034 (2022).
12. Peng, R. et al. Engineering a 3D DNA-Logic Gate Nanomachine for Bispecific Recognition and Computing on Target Cell Surfaces. *J Am Chem Soc* **140**, 9793-9796 (2018).
13. Tam, D.Y. et al. A Reversible DNA Logic Gate Platform Operated by One- and Two-Photon Excitations. *Angew Chem Int Ed Engl* **55**, 164-168 (2016).
14. Wang, D., Li, S., Zhao, Z., Zhang, X. & Tan, W. Engineering a Second-Order DNA Logic-Gated Nanorobot to Sense and Release on Live Cell Membranes for Multiplexed Diagnosis and Synergistic Therapy. *Angew Chem Int Ed Engl* **60**, 15816-15820 (2021).
15. Zhao, S. et al. Boolean logic gate based on DNA strand displacement for biosensing: current and emerging strategies. *Nanoscale Horiz* **6**, 298-310 (2021).
16. Liu, L., Liu, P., Ga, L. & Ai, J. Advances in Applications of Molecular Logic Gates. *ACS Omega* **6**, 30189-30204 (2021).
17. Alshangiti, D.M., Ghobashy, M.M., Alqahtani, H.A., El-damhougy, T.K. & Madani, M. The energetic and physical concept of gold nanorod-dependent fluorescence in cancer treatment and development of new photonic compounds|review. *RSC Advances* **13**, 32223-32265 (2023).
18. Chen, Z. et al. De novo design of protein logic gates. *Science* **368**, 78-84 (2020).
19. Zhang, F., Nangreave, J., Liu, Y. & Yan, H. Structural DNA Nanotechnology: State of the Art and Future Perspective. *J Am Chem Soc* **136**, 11198-11211 (2014).
20. Song, T. et al. Fast and compact DNA logic circuits based on single-stranded gates using strand-displacing polymerase. *Nature Nanotechnology* **14**, 1075-1081 (2019).
21. Simmel, F.C., Yurke, B. & Singh, H.R. Principles and Applications of Nucleic Acid Strand Displacement Reactions. *Chem Rev* **119**, 6326-6369 (2019).
22. Zhang, D.Y. & Seelig, G. Dynamic DNA nanotechnology using strand-displacement reactions. *Nat Chem* **3**, 103-113 (2011).
23. Riley, R.S. & Day, E.S. Gold nanoparticle-mediated photothermal therapy: applications and opportunities for multimodal cancer treatment. *Wiley Interdiscip Rev Nanomed Nanobiotechnol* **9** (2017).
24. Zhou, R. et al. Gold Nanorods-Based Photothermal Therapy: Interactions Between Biostructure, Nanomaterial, and Near-Infrared Irradiation. *Nanoscale Res Lett* **17**, 68 (2022).
25. Zhang, F. et al. Recent advances and mechanisms of action of PD-L1 degraders as potential therapeutic agents. *Eur J Med Chem* **268**, 116267 (2024).
26. Peng, Y. et al. An angel or a devil? Current view on the role of CD8(+) T cells in the pathogenesis of myasthenia gravis. *J Transl Med* **22**, 183 (2024).
27. Jelokhani-Niaraki, M. Membrane Proteins: Structure, Function and Motion. *International Journal of Molecular Sciences* **24**, 468 (2023).
28. Errasti-Murugarren, E., Bartoccioni, P. & Palacín, M. Membrane Protein Stabilization Strategies for Structural and Functional Studies. *Membranes* **11**, 155 (2021).
29. Seddon, A.M., Curnow, P. & Booth, P.J. Membrane proteins, lipids and detergents: not just a soap opera. *Biochimica et Biophysica Acta (BBA) - Biomembranes* **1666**, 105-117 (2004).
30. Hagn, F., Etzkorn, M., Raschle, T. & Wagner, G. Optimized Phospholipid Bilayer Nanodiscs Facilitate High-Resolution Structure Determination of Membrane Proteins. *J Am Chem Soc* **135**, 1919-1925 (2013).
31. González-Rubio, G. et al. Disconnecting Symmetry Breaking from Seeded Growth for the Reproducible Synthesis of High Quality Gold Nanorods. *ACS Nano* **13**, 4424-4435 (2019).